

Supporting Information

Dual Phosphorescence from the organic and inorganic moieties of 1D Hybrid Perovskites of the $\text{Pb}_{n'}\text{Br}_{4n'+2}$ Series ($n' = 2, 3, 4, 5$)

Maroua Ben Haj Salah,^{a,b} Nicolas Mercier,^{*a} Magali Allain,^a Nabil Zouari^b and Chiara Botta^{*c}

^a MOLTECH Anjou, UMR-CNRS 6200, Université d'Angers, 2 Bd Lavoisier, 49045 Angers, France

^b Laboratoire de Physico-chimie de l'état solide, Département de chimie, Faculté des sciences de SFax, B.P 1171, 3000, SFAX, Université de SFax, Tunisia.

^c Istituto per lo Studio delle Macromolecole (ISMAC), CNR. Via Corti 12, 20133 Milano, Italy.

Table of contents

Table S1, Summary of crystallographic data of compound 1

Table S2, Summary of crystallographic data of compound 2

Table S3, Summary of crystallographic data of compound 3

Table S4, Summary of crystallographic data of compound 4

Table S5 Emission properties of the four compounds as crystallized powders, compound 2 cast film and organic salts

Figure S1- Powder X-ray diffraction of compound 1

Figure S2- Powder X-ray diffraction of compound 2

Figure S3- Powder X-ray diffraction of compound 3

Figure S4- Powder X-ray diffraction of compound 4

Fig.S5. PL decay of compound 1, at RT, exc 408nm

Fig.S6 PL decay of compound 1, at RT, exc 300 nm

Fig.S7 Ph decay of compound 1, at RT

Fig.S8 PL decay of compound 2, at RT.

Fig.S9 Ph decay of compound 2 at RT.

Fig.S10 PL time decay of compound 3.

Fig.S11 Ph time decay of compound 3.

Fig.S12 PL time decay of compound 4.

Fig.S13 Ph time decay of compound 4.

Fig.S14 Temperature evolution of the emission of compound 2 .

Fig.S15 PL time decay of compound 2 at LT, exc 408nm.

Fig.S16 PL time decay of compound 2 at LT, exc 300nm.

Fig.S17 PL and Ph properties of Lysine Cl salt at RT

Fig.S18 PL time decay of Lysine Cl salt.

Fig.S19 Ph time decay of Lysine Cl salt.

Fig.S20 PL and Ph properties of Lysine Br salt.

Fig.S21 Ph time decay of Lysine Br salt.

Fig.S22 Ph time decay of Ornithine Cl salt.

Fig.S23 Optical absorption of cast film of compound 2

Fig.S24 PL time decay of film of compound 2 , RT.

Fig.S25 Ph time decay of film of compound 2 , RT.

Fig.S26 PL time decay of film of compound 2 at different temperatures.

Fig.S27 Ph time decay of film of compound 2 at LT.

**Table S1- Summary of crystallographic data and structure refinements of
 $(C_6H_{16}N_2O_2)_3Pb_2Br_{10} \cdot 3H_2O$ (1)**

| | |
|---------------------------------|---|
| Empirical formula | C18 H48 Br10 N6 O9 Pb2 |
| Formula weight | 1712.02 |
| Temperature | 150(10) K |
| Wavelength | 1.54184 Å |
| Crystal system, space group | Monoclinic, P 21 |
| Unit cell dimensions | a = 8.1393(3) Å alpha = 90 deg. b = 25.2015(9) Å beta = 91.088(3) deg. c = 10.9881(5) Å gamma = 90 deg. |
| Volume | 2253.50(15) Å^3 |
| Z, Calculated density | 4, 2.514 Mg/m^3 |
| Absorption coefficient | 25.119 mm^-1 |
| F(000) | 1568 |
| Theta range for data collection | 3.508 to 72.633 deg. |
| Limiting indices | -10<=h<=8, -30<=k<=30, -11<=l<=13 |
| Reflections collected / unique | 9248 / 6698 [R(int) = 0.0636] |
| Completeness to theta = 69.000 | 99.5 % |
| Refinement method | Full-matrix least-squares on F^2 |
| Data / restraints / parameters | 6698 / 1 / 404 |
| Goodness-of-fit on F^2 | 1.013 |
| Final R indices [I>2sigma(I)] | R1 = 0.0576, wR2 = 0.1458 |
| R indices (all data) | R1 = 0.0684, wR2 = 0.1516 |
| Absolute structure parameter | -0.023(15) |
| Extinction coefficient | 0.00007(5) |
| Largest diff. peak and hole | 2.190 and -2.268 e.Å^-3 |

**Table S2- Summary of crystallographic data and structure refinements of
 $(C_5H_{15}N_2O_2)_4Pb_3Br_{14}\cdot 2H_2O$ (2)**

| | |
|-----------------------------------|--|
| Empirical formula | C20 H64 Br14 N8 O10 Pb3 |
| Formula weight | 2317.10 |
| Temperature | 150(10) K |
| Wavelength | 1.5418 Å |
| Crystal system, space group | Triclinic, P 1 |
| Unit cell dimensions | a = 8.274(5) Å alpha = 71.769(5) deg. b = 11.580(5) Å beta = 77.947(5) deg. c = 15.717(5) Å gamma = 72.105(5) deg. |
| Volume | 1350.5(11) Å ³ |
| Z, Calculated density | 1, 2.849 Mg/m ³ |
| Absorption coefficient | 30.423 mm ⁻¹ |
| F(000) | 1056 |
| Theta range for data collection | 2.983 to 72.610 deg. |
| Limiting indices | -10<=h<=10, -14<=k<=13, -19<=l<=19 |
| Reflections collected / unique | 22457 / 9754 [R(int) = 0.0482] |
| Completeness to theta = 70.000 | 99.4 % |
| Refinement method | Full-matrix least-squares on F ² |
| Data / restraints / parameters | 9754 / 9 / 494 |
| Goodness-of-fit on F ² | 1.015 |
| Final R indices [I>2sigma(I)] | R1 = 0.0306, wR2 = 0.0738 |
| R indices (all data) | R1 = 0.0325, wR2 = 0.0745 |
| Absolute structure parameter | 0.011(7) |
| Extinction coefficient | 0.00015(2) |
| Largest diff. peak and hole | 1.310 and -1.415 e.Å ⁻³ |

**Table S3- Summary of crystallographic data and structure refinements of
 $(C_6H_{16}N_2O_2)_6Pb_4Br_{18} \cdot 2Br \cdot 2H_2O$ (3)**

| | |
|-----------------------------------|---|
| Empirical formula | C36 H100 Br20 N12 O14 Pb4 |
| Formula weight | 3352.24 |
| Temperature | 150.0(1) K |
| Wavelength | 1.54184 Å |
| Crystal system, space group | Monoclinic, P 21 |
| Unit cell dimensions | a = 12.3316(4) Å alpha = 90 deg. b = 8.0863(2) Å beta = 101.621(3) deg. |
| | c = 23.0098(7) Å gamma = 90 deg. 2247.44(12) Å ³ |
| Volume | 1, 2.477 Mg/m ³ |
| Z, Calculated density | 25.132 mm ⁻¹ |
| Absorption coefficient | 1540 |
| F(000) | 0.243 x 0.097 x 0.042 mm |
| Crystal size | 3.788 to 72.403 deg. |
| Theta range for data collection | -13<=h<=14, -6<=k<=9, - |
| Limiting indices | |
| 26<=l<=28 | |
| Reflections collected / unique | 9202 / 5750 [R(int) = 0.0483] |
| Completeness to theta = 70.000 | 99.3 % |
| Absorption correction | Semi-empirical from equivalents |
| Max. and min. transmission | 1.00000 and 0.58612 |
| Refinement method | Full-matrix least-squares on |
| F ² | |
| Data / restraints / parameters | 5750 / 33 / 418 |
| Goodness-of-fit on F ² | 1.004 |
| Final R indices [I>2sigma(I)] | R1 = 0.0599, wR2 = 0.1649 [5471 |
| Fo] | |
| R indices (all data) | R1 = 0.0621, wR2 = 0.1686 |
| Absolute structure parameter | -0.027(14) |
| Largest diff. peak and hole | 3.787 and -3.426 e.Å ⁻³ |

**Table S4- Summary of crystallographic data and structure refinements of
 $(C_6H_{16}N_2O_2)_6Pb_5Br_{22} \cdot 4H_2O$ (4)**

| | |
|---------------------------------|--|
| Empirical formula | C36 H104 Br22 N12 O16 Pb5 |
| Formula weight | 3755.28 |
| Temperature | 150.0(1) K |
| Wavelength | 1.54184 Å |
| Crystal system, space group | Monoclinic, P 21/c |
| Unit cell dimensions | a = 26.7956(13) Å alpha = 90 deg. b = 8.1729(3) Å beta = 112.775(6) deg. |
| | c = 22.9805(11) Å gamma = 90 deg. |
| Volume | 4640.3(4) Å^3 |
| Z, Calculated density | 2, 2.688 Mg/m^3 |
| Absorption coefficient | 28.828 mm^-1 |
| F(000) | 3424 |
| Crystal size | 0.31 x 0.084 x 0.062 mm |
| Theta range for data collection | 3.578 to 72.669 deg. |
| Limiting indices | -32<=h<=28, -6<=k<=9, -28<=l<=28 |
| Reflections collected / unique | 18103 / 8948 [R(int) = 0.0635] |
| Completeness to theta = 71.500 | 98.4 % |
| Absorption correction | Semi-empirical from equivalents |
| Max. and min. transmission | 1.00000 and 0.58122 |
| Refinement method | Full-matrix least-squares on F^2 |
| Data / restraints / parameters | 8948 / 36 / 419 |
| Goodness-of-fit on F^2 | 0.988 |
| Final R indices [I>2sigma(I)] | R1 = 0.0499, wR2 = 0.1100 [6517 fo] |
| R indices (all data) | R1 = 0.0775, wR2 = 0.1248 |
| Largest diff. peak and hole | 2.326 and -2.762 e.Å^-3 |

Table S5 Emission properties of the four compounds as crystallized powders, compound 2 cast film and organic salts

| | Abs λ_{\max} (nm) | PL Excitation λ_{\max} (nm) | PL Emission λ_{\max} (nm) | QY (%) | PL τ_{av} (ns) exc300 | Ph Excitation λ_{\max} (nm) | Ph Emission λ_{\max} (nm) | Phos τ_{av} (ms) |
|--------------------------------------|---------------------------|--|-----------------------------------|-----------|----------------------------|-------------------------------------|--|-----------------------|
| 1 | | 290,320, 356 380, 402 ^{sh} | 635 398,418,440 | 0.10 | < 0.3 (390) 1.06 (418) | 380 420 440 480 | 570 (exc380) 590 (exc408) 630 (exc420) 710 (exc480) | 4.66 4.43 |
| 2 cryst RT | | 295,335,366, | 390, 545 | 13.4 6 | 16.5 (390) 97.8 (560) | 394 421 | 557 (exc393) 595 (exc422) 570 (exc365) | 10.93 5.99 2.80 |
| 2 cryst LT | | 290,340,357,398, | 570 | | 5.25 (410) 76.63 (570) | 280, 395 | 400 (exc300) 600 (exc300) 590 (exc390) | 19.09 11.84 |
| 2 film RT | 260,316, 388 | 287,402 284,371 | 404, 560 | | 3.13 | 362,406 | 610 (ex340,400) 595 (exc300) | 1.26- 2.46 |
| 2 film LT | | 277,316,388 277,348,376,401 | 402, 620 | | 3.82 (403) 48.64 (620) | 287,395 | 403 620 | 5.47 4.87 |
| 3 | | 275, 345, 375 | 390-420 , 575 | 27.7 4 | 20.4 (390) 36.0 (575) | 395, 386, 422 ^{sh} | 520(exc395) 600 (exc422) | 5.34 3.35 |
| 4 | | 280,380 | 410, 560 | 8.50 | 12.3 (400) 3449 (555) | 395, 417 | 560 | 4.27 |
| H₂Orn²⁺ | | 275, 410-420 | 490-515 | <0.1 | 3.9 (480em) | 295, 360 | 530-570 | 43 |
| H₂Lys²⁺ | | 280, 365 | 390-415 575 | <0.1 | 19.7-24.5 3.23 (575) | 293, 360 | 515 520 (Br salt) | 69 6.2 (Br salt) |

$$\tau_{av} = \sum_i \frac{A_i \tau_i^2}{A_i \tau_i}$$

$$\langle \tau \rangle = \sum_i \frac{A_i \tau_i}{A_i}$$

Figure S1- Powder X-ray diffraction of $(C_6H_{16}N_2O_2)_3Pb_2Br_{10} \cdot 3H_2O$ (1) : experimental (crystallized powder) and theoretical

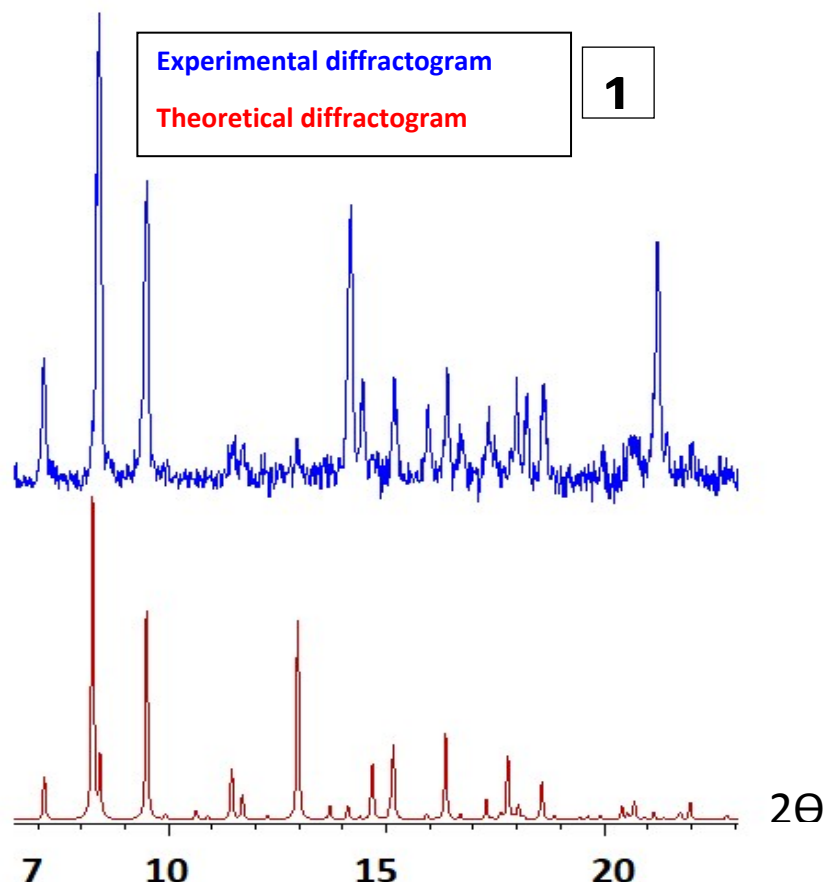


Figure S2- Powder X-ray diffraction of $(C_5H_{15}N_2O_2)_4Pb_3Br_{14}\cdot 2H_2O$ (2) : experimental (crystallized powder) and theoretical

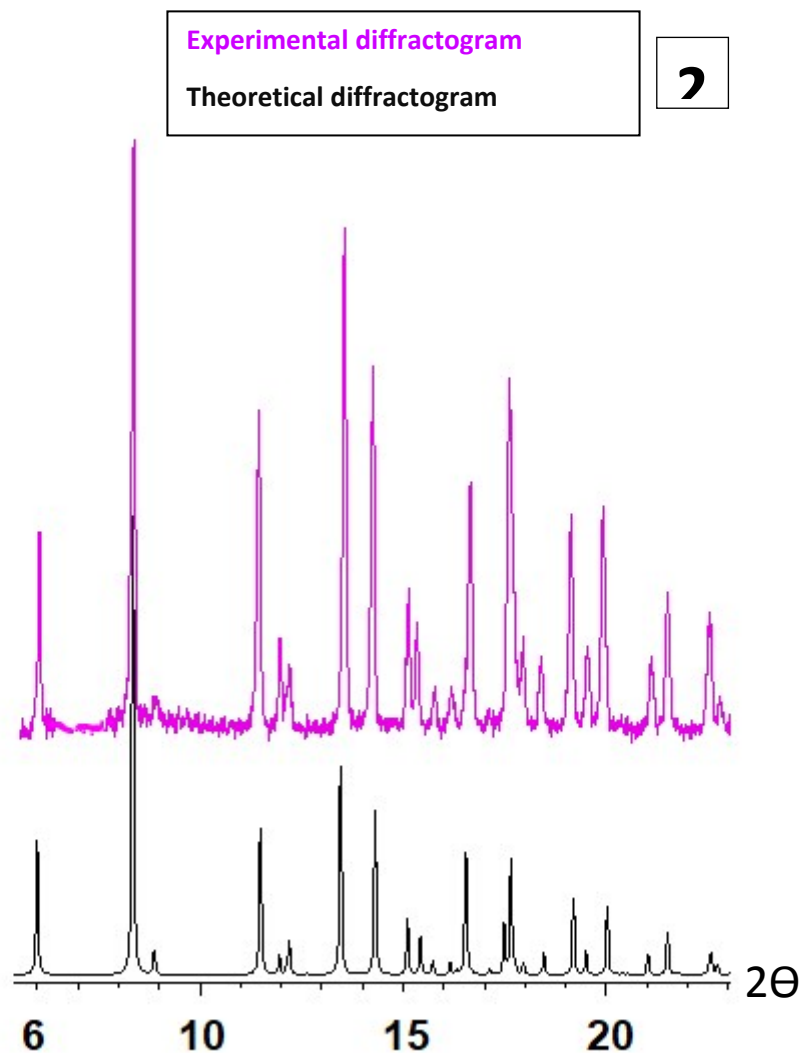


Figure S3- Powder X-ray diffraction of $(C_6H_{16}N_2O_2)_6Pb_4Br_{18} \cdot 2Br \cdot 2H_2O$ (3) : experimental (crystallized powder) and theoretical

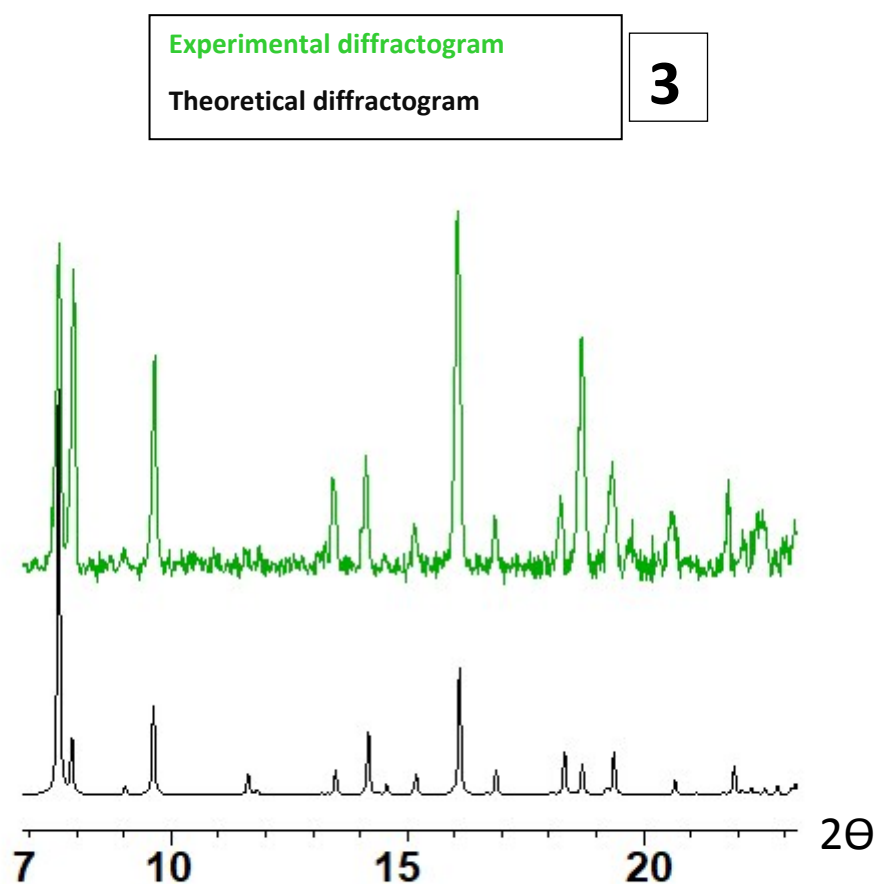
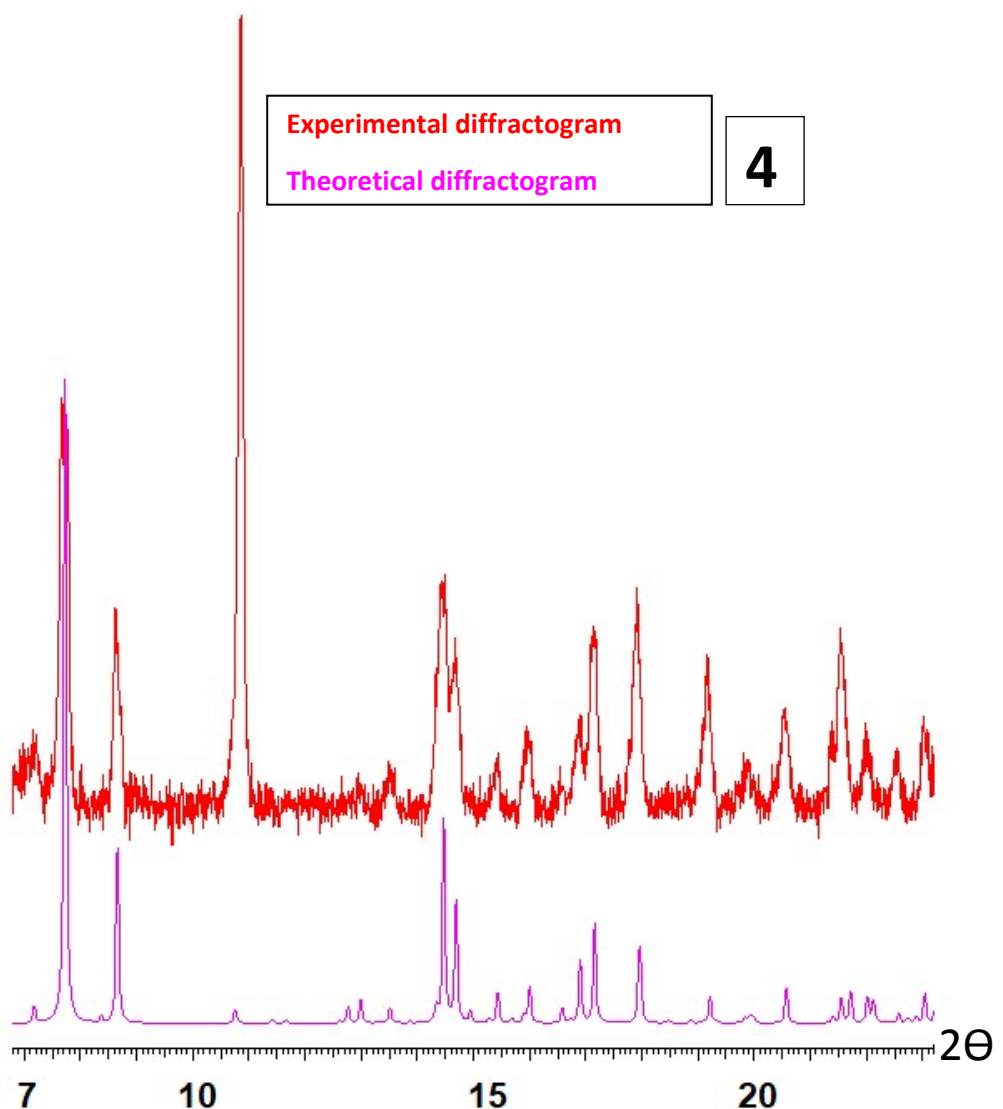


Figure S4- Powder X-ray diffraction of $(C_6H_{16}N_2O_2)_6Pb_5Br_{22} \cdot 4H_2O$ (4) : experimental (crystallized powder) and theoretical



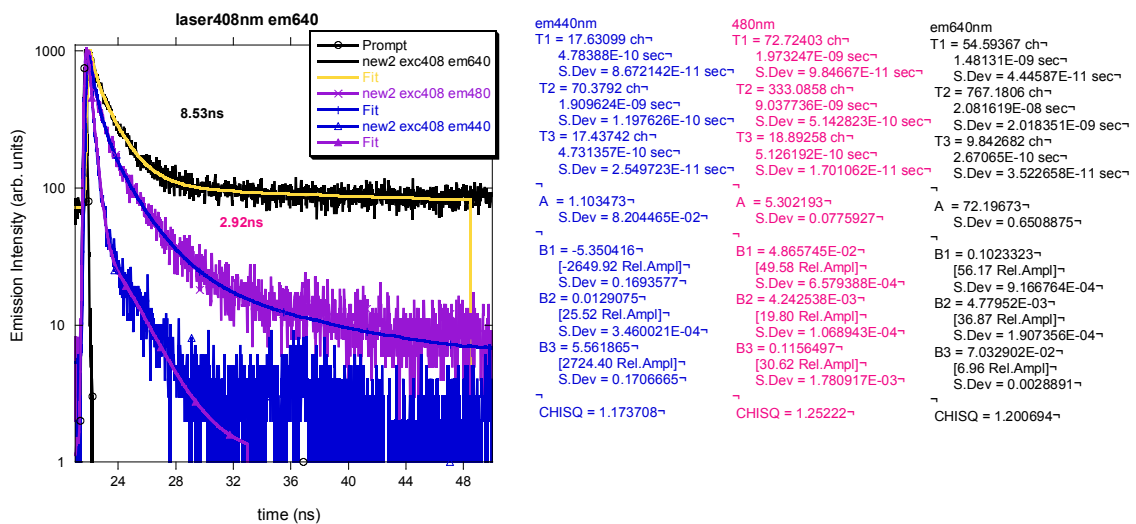
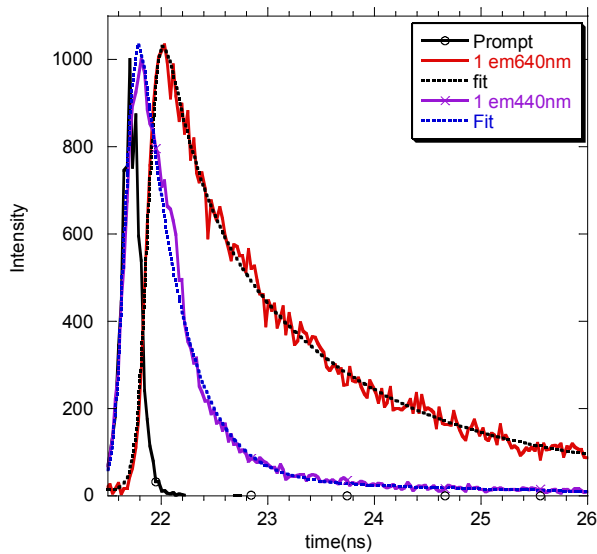


Fig.S5 PL decay of compound **1**, at RT, exc 408nm, emission at 640nm, 440nm and 480nm. 3exp fit: (480nm: $\langle\tau\rangle=1.159$ ns; $\tau_{av}=2.92$ ns; 560nm: $\langle\tau\rangle=1.52$ ns; $\tau_{av}=8.53$ ns)

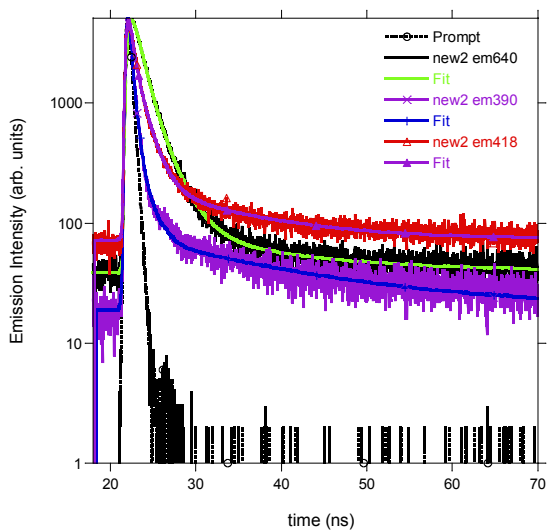


Fig.S6 PL decay of compound **1**, at RT, exc 300 nm, emission at 640, 390 and 418nm, with 3exp fits (418nm: $\langle\tau\rangle=0.31\text{ns}$; $\tau_{av}=1.06\text{ns}$; 560nm: $\langle\tau\rangle=1.14\text{ns}$; $\tau_{av}=2.45\text{ ns}$).

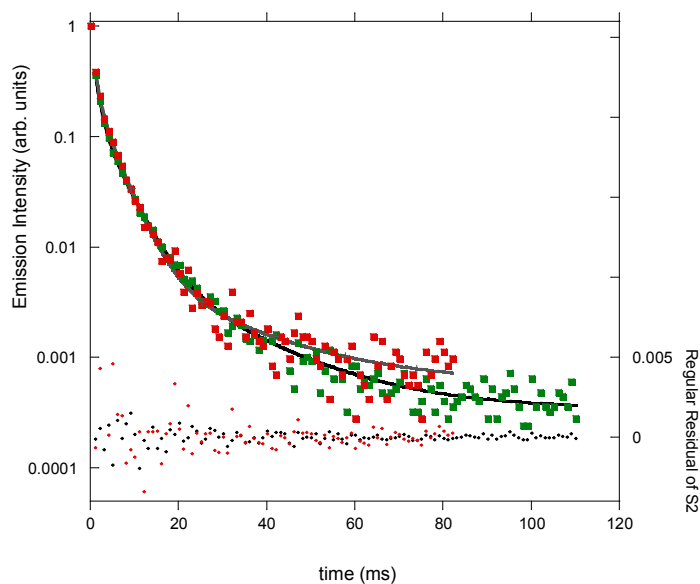
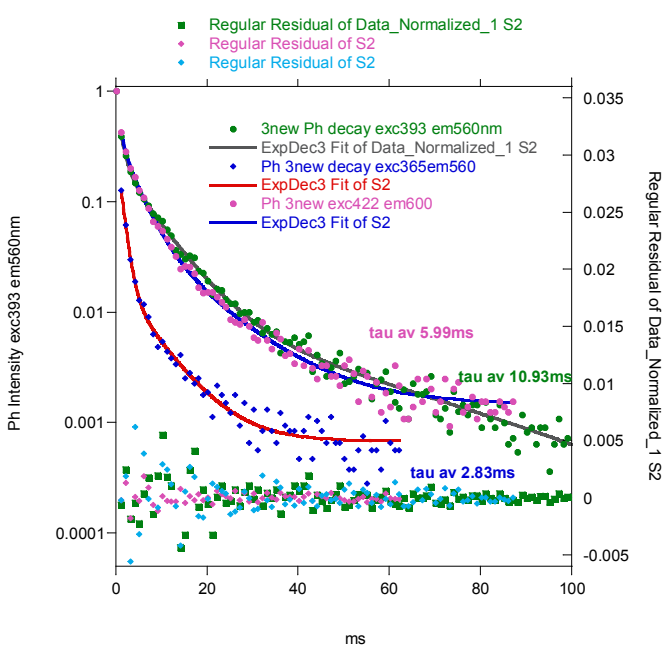
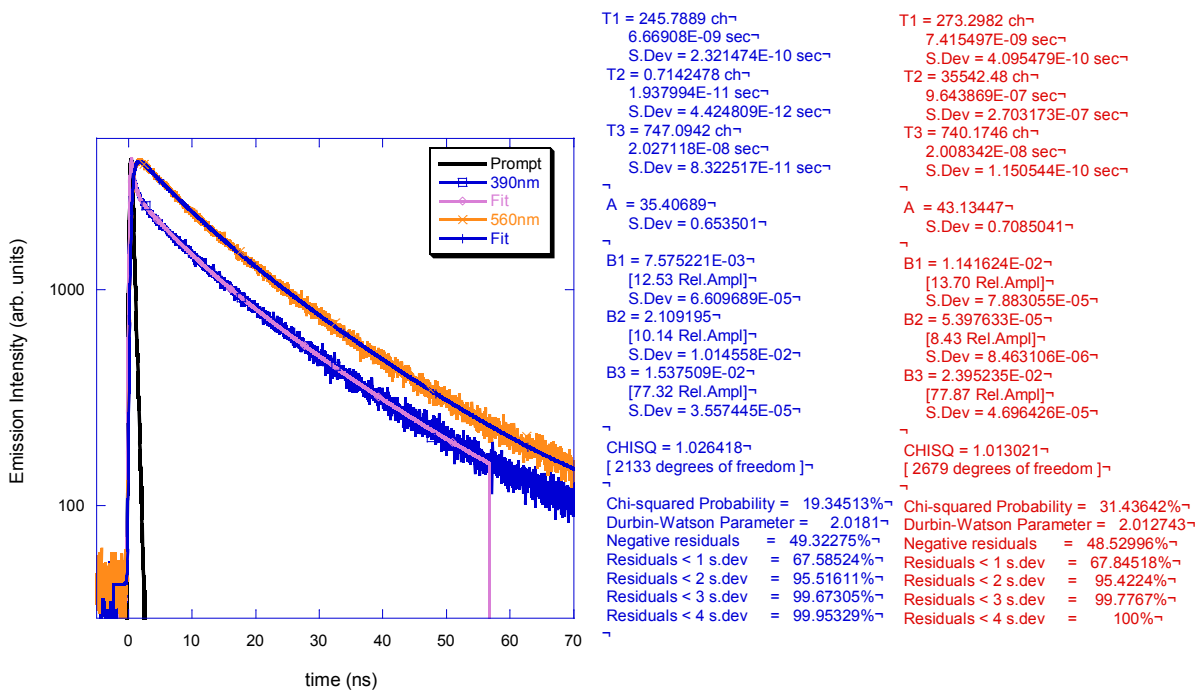


Fig.S7 Ph decay of compound **1**, at RT, exc 380 nm (emission at 600nm, $\tau_{av}=4.66\text{ms}$), exc 420 (emission at 640nm $\tau_{av}=4.43\text{ms}$).



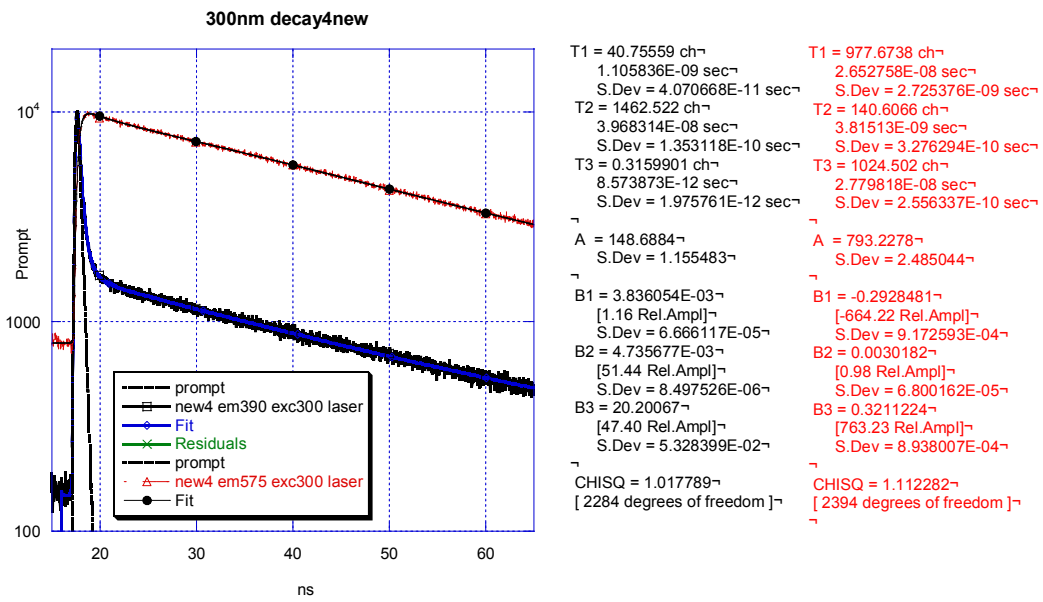


Fig.S10 PL time decay of compound **3**, exc300nm em390nm and 575nm. Emission at 390nm: $\langle\tau\rangle=0.02\text{ns}$, $\tau_{av}=20.43\text{ ns}$; Emission at 575nm: ns $\tau_{av}=36.00\text{ ns}$;

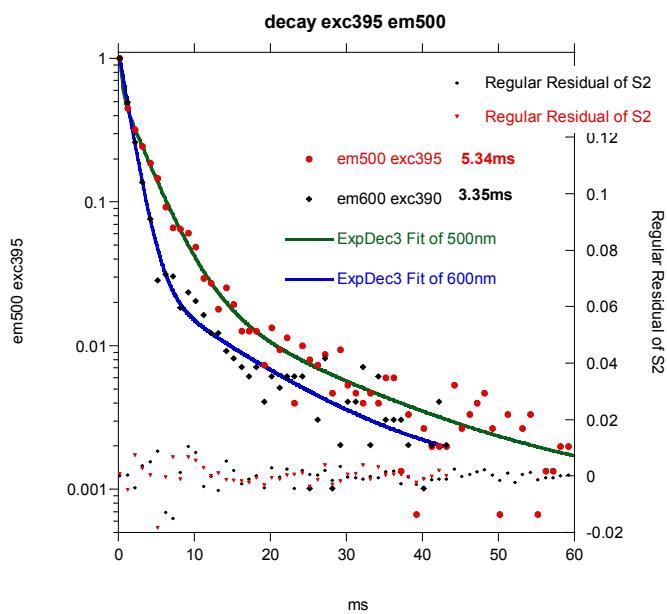


Fig.S11 Ph time decay of compound **3**, at RT, exc395nm em500nm; exc390 em600.

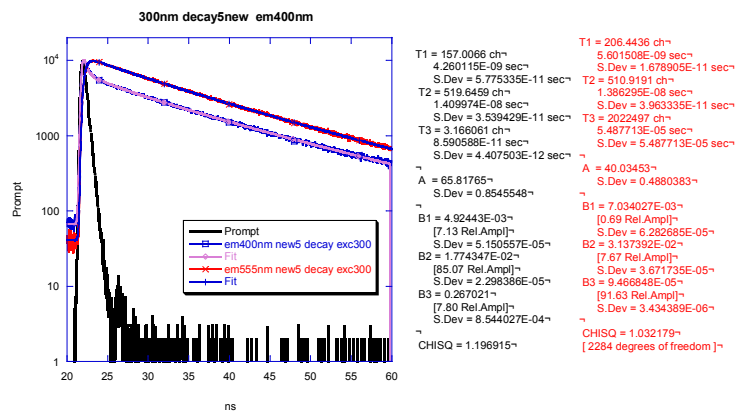


Fig.S12 PL time decay of compound **4**, exc300nm emission at 400nm and 555nm. Emission at 400nm: $\langle\tau\rangle=1\text{ ns}$, $\tau_{av}=12.30\text{ ns}$; Emission at 555nm: ns $\langle\tau\rangle=21.35\text{ ns}$ $\tau_{av}=3449\text{ ns}$;

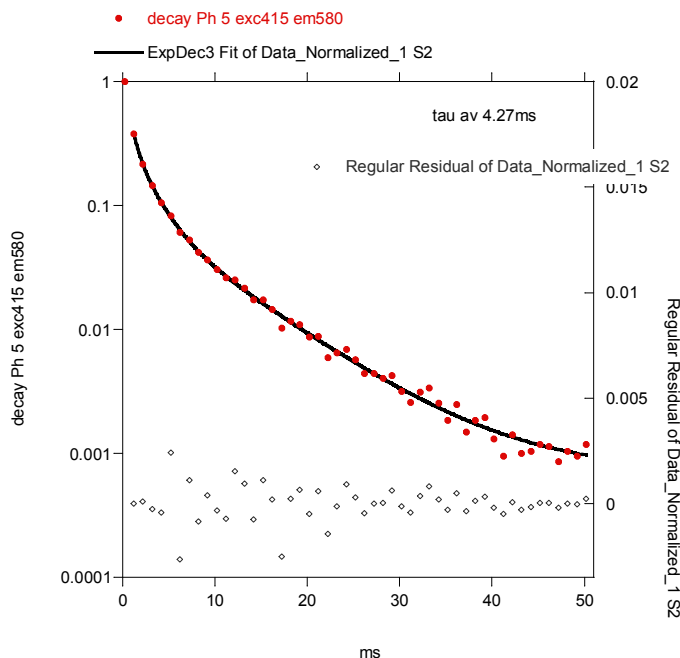


Fig.S13 Ph time decay of compound **4**, exc415nm, em580nm

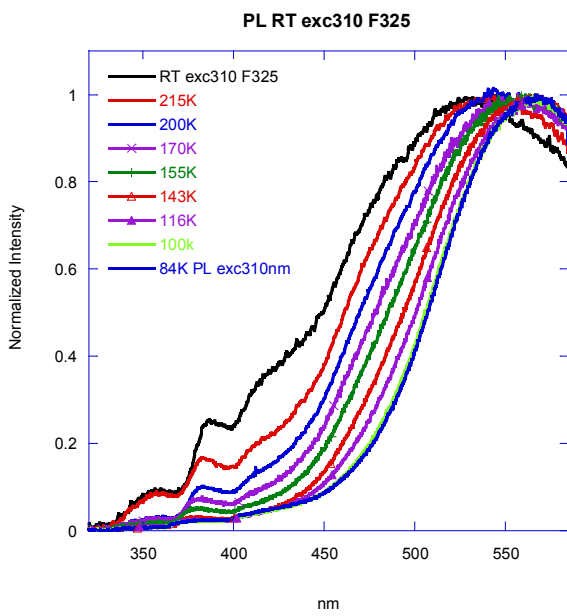


Fig.S14 Temperature evolution of the emission of compound **2** crystal powders. Normalized spectra.

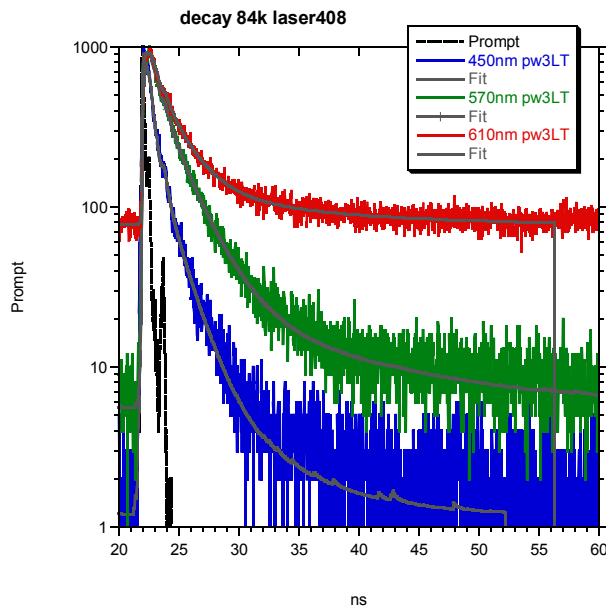


Fig.S15 PL time decay of compound **2** at LT, exc 408nm. 3exp fit: Emission at 450nm: $\langle\tau\rangle=0.55\text{ns}$, $\tau_{av}=1.13\text{ ns}$; 610nm: $\langle\tau\rangle=1.68\text{ns}$; ns $\tau_{av}=4.0\text{ ns}$;

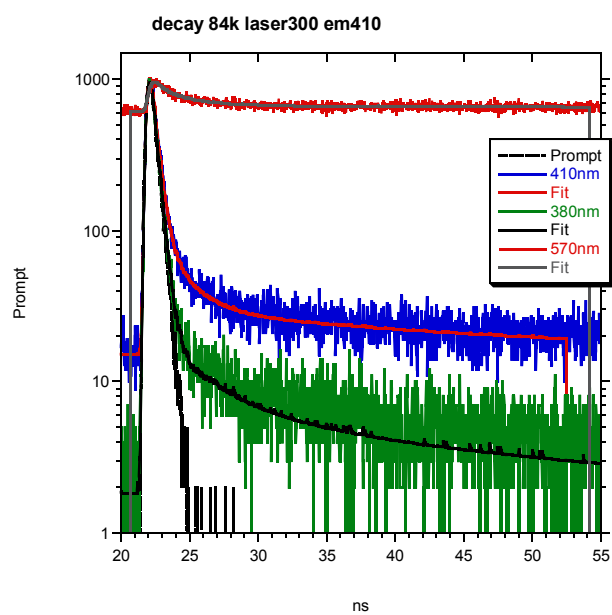
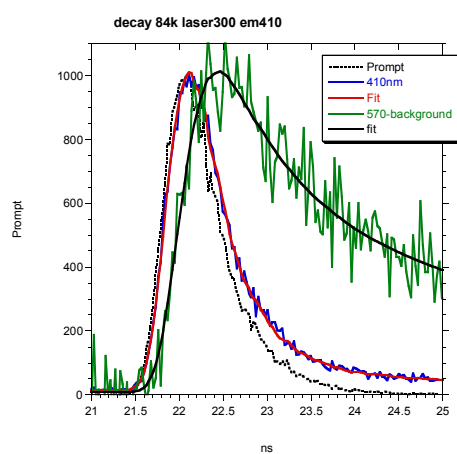


Fig.S16 PL time decay of compound **2** at LT, exc 300nm. Emission at 410nm: $\langle\tau\rangle=0.07\text{ns}$, $\tau_{av}=5.25\text{ ns}$; 570nm: $\langle\tau\rangle=5.49\text{ns}$; $\tau_{av}=76.63\text{ ns}$;

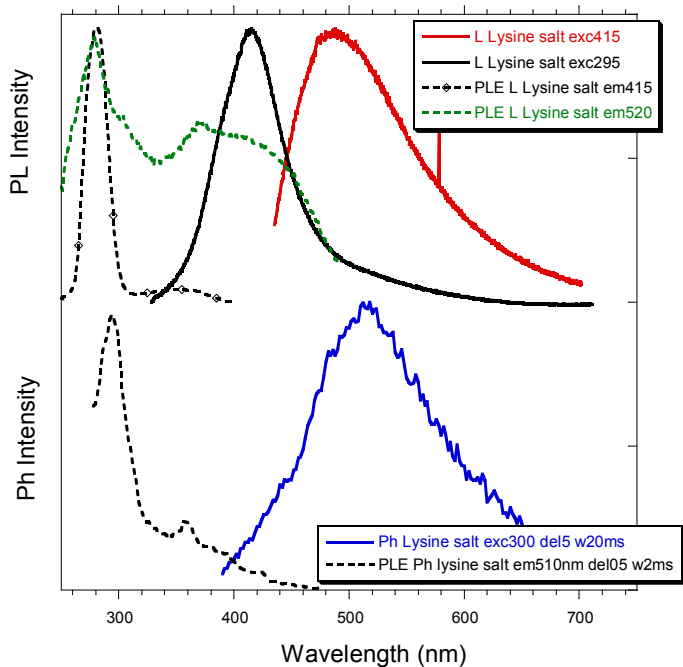


Fig.S17 PL and Ph properties of Lysine Cl salt at RT

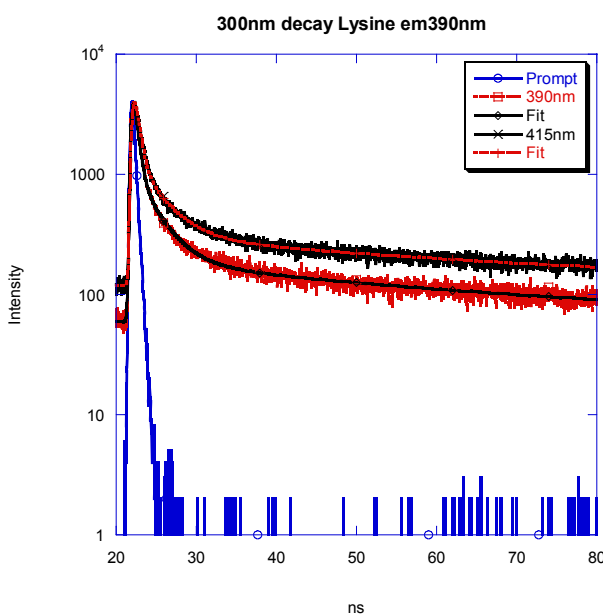


Fig.S18 PL time decay of Lysine Cl salt, exc300nm, emission at 390nm $\langle\tau\rangle=1.04\text{ns}$, $\tau_{av}=19.69\text{ns}$; . Emission at 415nm: $\langle\tau\rangle=1.65\text{ns}$ ns; $\tau_{av}=24.646\text{ns}$

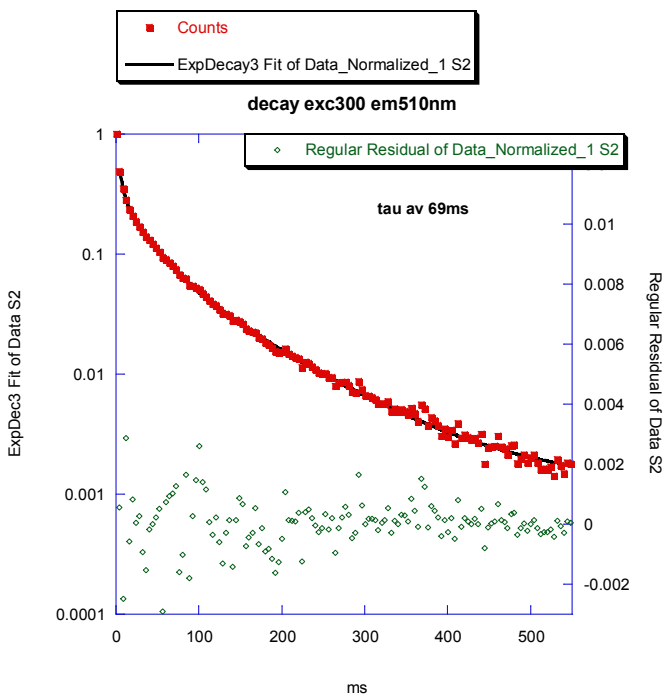


Fig.S19 Ph time decay of Lysine Cl salt, exc300nm, emission at 510nm

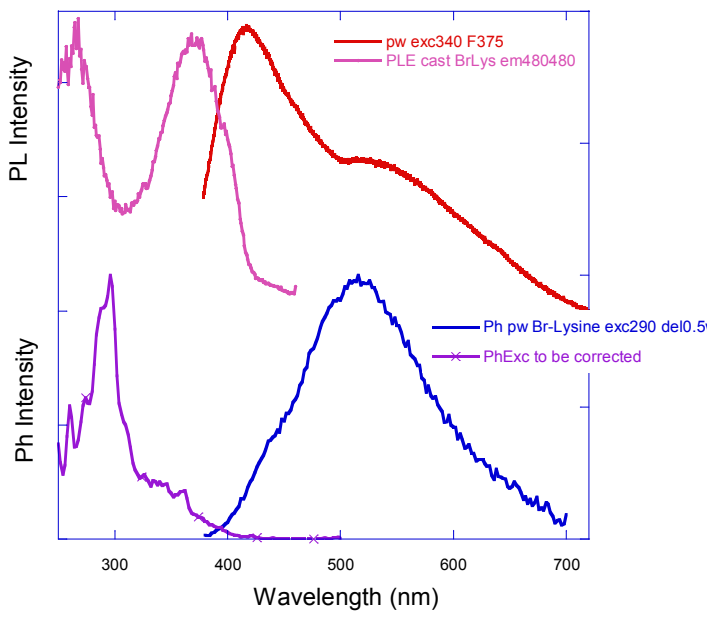


Fig.S20 PL and Ph properties of Lysine Br salt, at RT

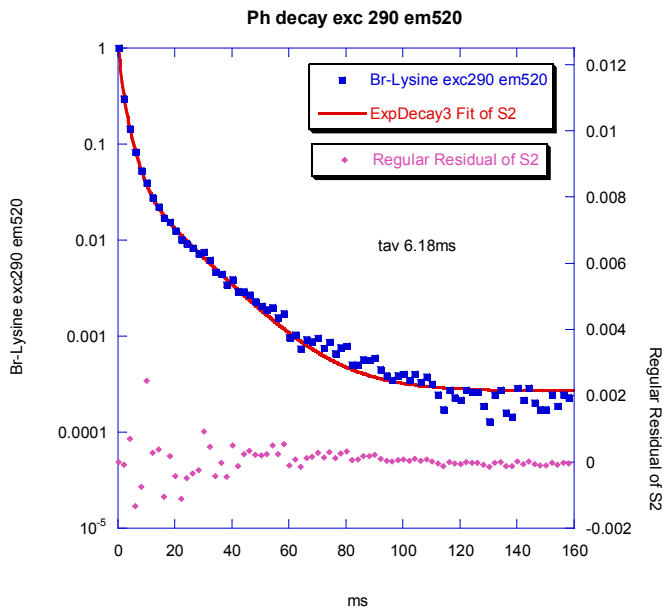


Fig.S21 Ph time decay of Lysine Br salt, exc 290nm emission 520nm

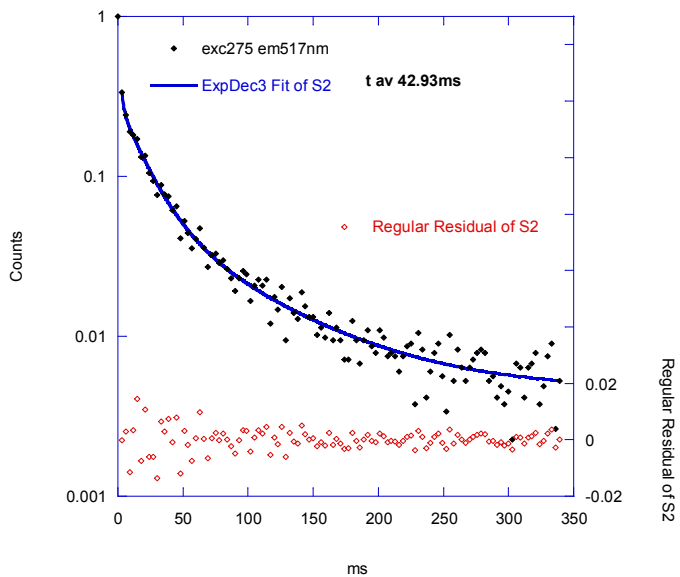


Fig.S22 Ph time decay of Ornithine Cl salt, exc275nm, emission at 517nm

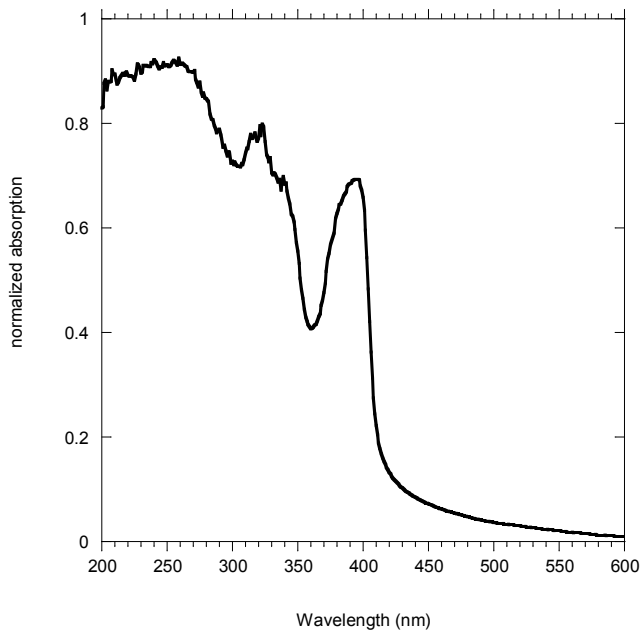


Fig.S23 Optical absorption of cast film of compound 2

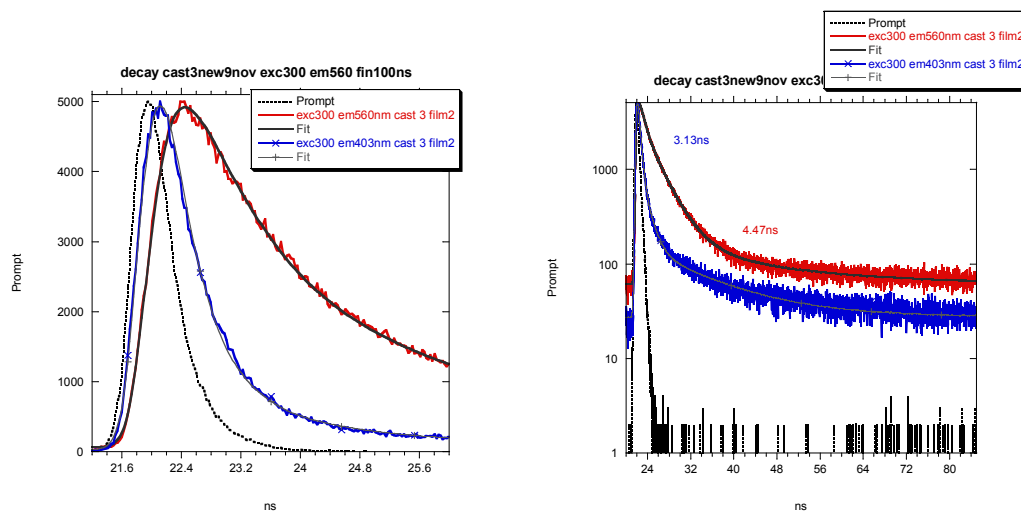


Fig.S24 PL time decay of film of compound 2 , RT, exc300nm. Emission 403nm $\langle\tau\rangle=0.35\text{ns}$, $\tau_{av} = 3.13\text{ ns}$; Emission 560nm $\langle\tau\rangle=1.96\text{ns}$, $\tau_{av} = 4.77 \text{ ns}$

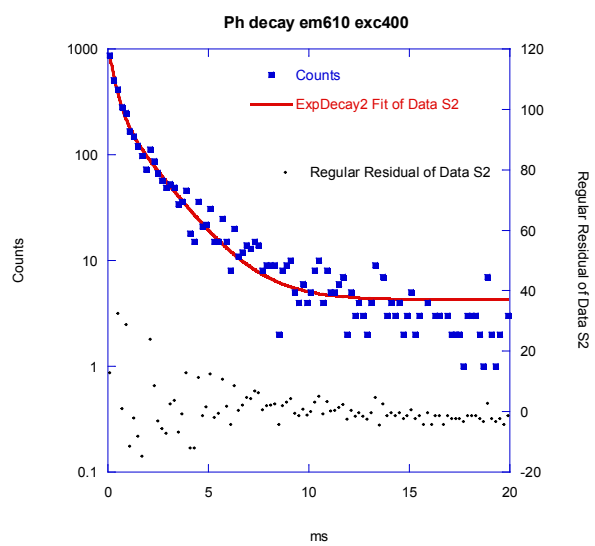


Fig.S25 Ph time decay of cast film of compound **2**, RT exc400nm, em610nm. $\tau_{av} = 1.26$ ms;

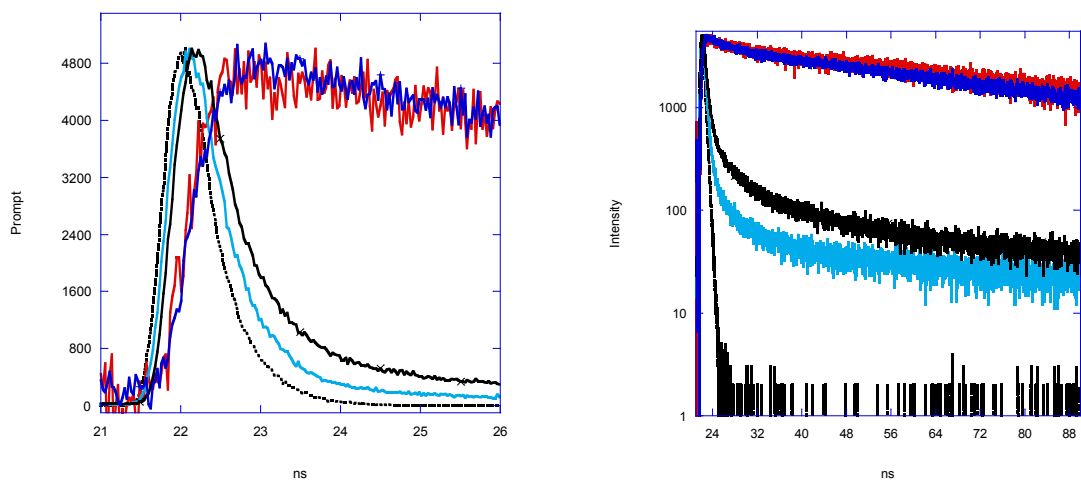


Fig.S26 PL time decay of cast film of compound **2** at different temperatures. T=845K, emission at 620nm and 403nm, red and cyan lines, respectively; T=132K, emission at 620nm and 403nm, blue and black lines, respectively. exc300nm.

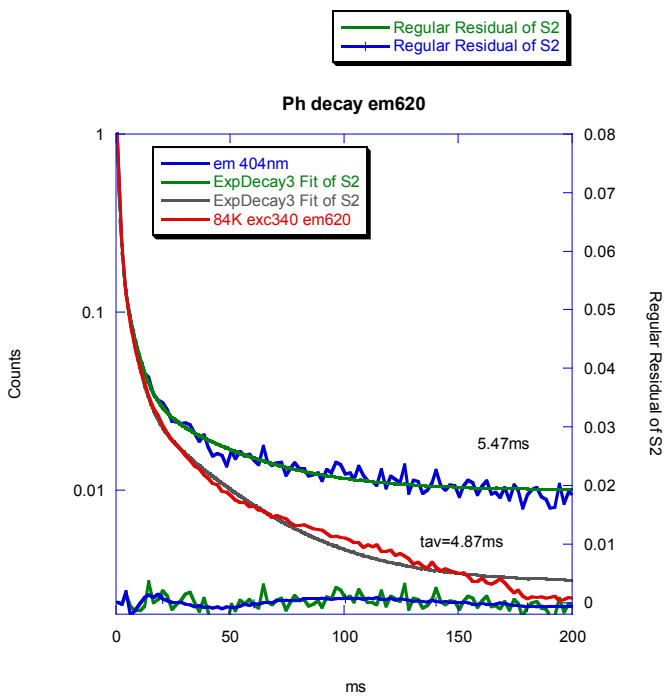


Fig.S27 Ph time decay of cast film of compound **2** at LT, exc300nm. Emission 404 nm $\tau_{av} = 5.47$ ms; Emission 620 nm $\tau_{av} = 4.87$ ms.